FEBS Letters 459 (1999) 438–442 FEBS 22686

A stability transition at mildly acidic pH in the alpha-hemolysin (alpha-toxin) from *Staphylococcus aureus*

Raquel Kely Bortoleto[a], Richard J. Ward[b,*]

[a] *Department of Physics, IBILCE/UNESP, Rua Cristovão Colombo 2265, São José do Rio Preto, SP, Brazil*
[b] *Department of Chemistry, Faculdade de Filosofia, Ciências e Letras de Ribeirão Preto-USP (FFCLRP), Avenida Bandeirantes 3900, Ribeirão Preto, SP, Brazil*

Received 30 August 1999; received in revised form 6 September 1999

Abstract The effects of mildly acidic conditions on the free energy of unfolding (ΔG_u^{buff}) of the pore-forming alpha-hemolysin (αHL) from *Staphylococcus aureus* were assessed between pH 5.0 and 7.5 by measuring intrinsic tryptophan fluorescence, circular dichroism and elution time in size exclusion chromatography during urea denaturation. Decreasing the pH from 7.0 to 5.0 reduced the calculated ΔG_u^{buff} from 8.9 to 4.2 kcal mol^{-1}, which correlates with an increased rate of pore formation previously observed over the same pH range. It is proposed that the lowered surface pH of biological membranes reduces the stability of αHL thereby modulating the rate of pore formation.

Key words: α-Hemolysin; Stability transition

1. Introduction

Alpha-hemolysin (αHL, also referred to as alpha-toxin) is a major exotoxin produced by pathogenic strains of the Gram-positive bacterium *Staphylococcus aureus*. The toxin is secreted as a hydrophilic monomer, which in vivo binds to a receptor on target cell membranes, and oligomerizes to form a transmembrane pore (reviews [1,2]). At higher concentrations in vitro, αHL binds to artificial membranes and the investigation of this interaction has yielded detailed information concerning the pore-forming process [3]. Following initial membrane association, αHL undergoes a conformation conversion and oligomerizes to form a heptameric non-lytic pre-pore [4,5]. A subsequent conformation change in the pre-pore complex results in the formation of a fully lytic heptameric transmembrane pore [6,7]. A wealth of evidence has demonstrated that a central glycine rich region of the protein (residues 118–142) inserts into the membrane bilayer to form the walls of the pore, with the bulk of the heptamer remaining exposed to the solvent [8–16]. The crystal structure of the αHL heptamer reveals that the central glycine rich region from each monomer forms a two-stranded anti-parallel β-sheet which contributes to a 14-stranded β-barrel the lumen of which constitutes the transmembrane pore [17].

The factors which influence the conformation changes of the membrane associated αHL are poorly understood. The negatively charged phospholipid, glycolipid and glycoprotein contents of biological membranes result in the formation of an electrostatic double layer, where the concentrations of positively charged ions and protons are significantly higher at the membrane surface in relation to the bulk solvent (e.g. reviews [18,19]). Previous spectroscopic studies of αHL in solution have demonstrated that below pH 4.0 a biphasic structural transition occurs, during which the protein assumes properties consistent with those of a 'molten globule' state, and it has been suggested that reduced pH at the membrane surface may trigger a partial unfolding of αHL which in turn leads to pore formation [20,38]. This hypothesis may be feasible for model membranes with high negative surface charge densities (> -0.4 C m^{-2}); however, calculations based on Chapman-Gouy theory predict that negative charge densities similar to those in biological membranes (-0.05 to -0.1 C m^{-2}) result in a more modest pH reduction of 1.0–1.5 units in the region of the phospholipid headgroups relative to the bulk solvent [21–23]. These predictions have been confirmed experimentally both in model [22,24] and cell membranes [22]. Therefore, in order to determine the effects of pH changes over a physiological range, we have examined the thermodynamic stability of αHL using urea equilibrium unfolding as monitored by intrinsic tryptophan fluorescence, circular dichroism and size exclusion chromatography over the pH range 5.0–7.5.

2. Materials and methods

2.1. Protein purification

αHL was purified from culture supernatants of *S. aureus* strain Y1090 transformed with plasmid pDU1212 using a combination of ammonium sulfate precipitation and cation exchange chromatography as previously described [25]. Aliquots of purified protein were stored at −20°C for further use. Protein purity was routinely evaluated by silver staining of SDS-PAGE gels, which confirmed the protein remained in the monomeric state during purification and storage.

2.2. Intrinsic tryptophan fluorescence emission (ITFE) spectroscopy

αHL samples at a final concentration of 10 μg ml^{-1} were prepared in 20 mM acetate (pH 5.0 and 5.5) or 20 mM sodium phosphate (pH 6.0–7.5) buffers in the presence of 150 mM NaCl. For equilibrium denaturation experiments, the urea concentration in individual samples was increased over the range 0–6 M by dilution of a 10 M stock solution of re-crystallized urea prepared in the same buffer at the given pH. ITFE spectra were measured in the wavelength range 310–450 nm using a Hitachi F2000 spectrofluorimeter, with an excitation wavelength of 295 nm and excitation and emission slits set at 5 nm. Experiments were performed at 298 K, and all spectra were corrected by subtraction of the spectrum from the equivalent buffer at the given urea concentration. The observed spectral centers of mass, C_M^{obsd}, of the ITFE spectra were calculated according to:

$$C_M^{obsd} = \sum I_{\lambda^{-1}} \lambda^{-1} / \sum I_{\lambda^{-1}} \quad (1)$$

where $I_{\lambda^{-1}}$ is the fluorescence emission intensity at wavenumber λ^{-1}. These values of C_M^{obsd} were used to estimate the Gibbs free energy between the native and unfolded protein states (ΔG_U^{buff}) in buffers at

*Corresponding author. Fax: (55) (16) 6338151.
E-mail: rjward@fmrp.usp.br

PII: S0014-5793(99)01246-6

all pH values assuming a two-state unfolding model for a monomer [26,27]. In this model C_M^{obsd} is related to the denaturant concentration, [D], by the expression:

$$C_M^{obsd} = [(C_{MN}^0 + m_N[D]) + (C_{MU}^0 + m_U[D])K_U)]/(1 + K_U) \quad (2)$$

where C_{MN}^0 and C_{MU}^0 are the values of the intercepts, and m_N and m_U are the slopes of the linear pre- and post-transition phases in which the protein is present in the native and unfolded states respectively. The equilibrium constant for the transition between native and unfolded states, K_U, is calculated by:

$$K_U = \exp[-1 \times (\Delta G_U^{buff} - m_D[D])/RT] \quad (3)$$

where m_D is the slope describing the dependence of ΔG_U^{buff} on the denaturant concentration. Eqs. 2 and 3 were combined in a non-linear least squares fitting of C_M^{obsd} and [D] using C_{MN}^0, C_{MU}^0, m_N, m_U, m_D and ΔG_U^{buff} as fitting parameters. The accuracy of the fitting procedure was evaluated by manual input of varying values of the fitting parameters. Convergence of parameter values was unaffected by perturbations of ±10% in the initial values, above which convergence was only achieved at the expense of increased values of the standard error between the experimental and the fitted data.

2.3. Circular dichroism (CD)

Samples containing a final protein concentration of 10 μg ml^{-1} were prepared in buffers at pH 5.0 and 7.0 containing 0–6 M urea as described previously for the fluorescence experiments. The CD at 218 nm was measured with a Jasco 900 spectropolarimeter using 1 mm pathlength quartz cuvettes by integration of the signal over a 60 s period. The temperature was maintained constant at 298 K, and in all cases a correction was made by subtraction of the integrated signal measured from a buffer blank over the same time scale. The observed changes in the CD signal at 218 nm (C_D^{obsd}) as a function of urea concentration were analyzed using non-linear least squares fitting of Eqs. 2 and 3. The terms C_{MN}^0 and C_{MU}^0 in Eq. 2 were replaced by C_{DN}^0 and C_{DU}^0, the intercept values of the linear pre- and post-transition phases of the CD signal for the protein in the native and unfolded states respectively.

2.4. Size exclusion chromatography (SEC)

Unfolding of αHL was monitored by measuring the elution time using a Sepharose 6B (Pharmacia, Uppsala, Sweden) column (1.6 cm×35 cm) in pH 5.0 and 7.0 buffers during the application of a linear gradient of urea over the concentration range 0–6 M. αHL at a concentration of 2.0 mg ml^{-1} in the appropriate buffer without urea was injected in 100 μl aliquots at pre-determined time intervals during the gradient run. The application of the mobile phase was maintained at a constant rate of 0.3 ml min^{-1}, and the elution time of the protein was measured by continuously monitoring the A_{280} of the eluate.

3. Results

The ITFE spectra for native αHL over the pH range 5.0–7.5 show a constant maximum emission wavelength (λ_{max}) of 336 nm, which is consistent with previously reported values of the native protein [20,25]. In order to determine if a reduction in pH resulted in tertiary structure changes, both quenching of the ITFE by iodide and the quantum yield of aniline-8-sulfonic acid (ANS) were measured over the pH range 5.0–7.5. No significant changes were observed in either experiment, which confirms the results of previous investigations [20] and indicates that in the absence of urea no detectable changes in tertiary structure occur over the pH range studied. The addition of urea to a final concentration of 6 M results in a red shift in the λ_{max} to 352 nm with a concomitant decrease in emission intensity due to the increased exposure of tryptophans to the aqueous solvent. The red shift in the ITFE on addition of urea results in a decrease in the spectral center of mass (COM), and these data are represented in Fig. 1 as the fraction of native protein (f_{nat}) for experiments over the pH range 5.0–7.5. Fig. 1 includes both the experimentally determined values of f_{nat} and curves derived from the non-linear least squares fitting of the data using a two-state unfolding model for a monomer. At all pH values a clear transition between the native and unfolded states is observed, which occurs at progressively lower concentrations of urea as the pH is reduced from pH 7.5 to 5.0. The values derived for ΔG_u^{buff} and m_D from these unfolding curves are shown in Table 1. The αHL monomer contains eight Trp residues distributed both in the two principal domains (the so-called rim and cap domains, Trp residues are absent in the third transmembrane stem domain) and at the interface between these domains [17]. Changes in the microenvironments of all Trp

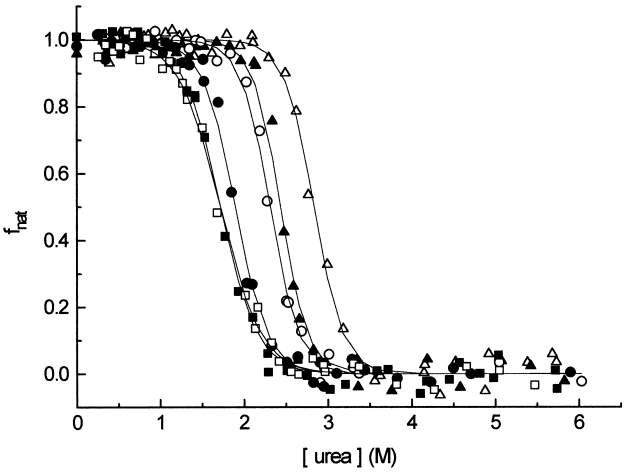

Fig. 1. Changes in the fraction of native αHL (f_{nat}) derived from ITFE data as a function of urea concentration at pH values of 5.0 (■), 5.5 (□), 6.0 (●), 6.5 (○), 7.0 (▲) and 7.5 (△). The solid lines in each case are the results of non-linear least squares fitting to the data used to derive the values of ΔG_U^{buff}, m_D, and $[urea]_{50}$.

Table 1
Values of ΔG_U^{buff}, m_D and $[urea]_{50}$ of αHL, over the pH range 5.0–7.5 measured changes in ITFE, CD and SEC

pH	ITFE			CD			SEC
	ΔG_U^{buff} (kcal mol^{-1})	m_D (kcal mol^{-1}M^{-1})	$[urea]_{50}$ (M)	ΔG_U^{buff} (kcal mol^{-1})	m_D (kcal mol^{-1} M^{-1})	$[urea]_{50}$ (M)	$[urea]_{50}$ (M)
5.0	4.2	2.4	1.7	4.1	2.5	1.6	1.7
5.5	4.7	2.7	1.7	n.d.	n.d.	n.d.	n.d.
6.0	5.9	3.1	1.9	n.d.	n.d.	n.d.	n.d.
6.5	8.0	3.4	2.3	n.d.	n.d.	n.d.	n.d.
7.0	8.9	3.7	2.4	8.9	3.7	2.4	2.6
7.5	9.7	3.4	2.8	n.d.	n.d.	n.d.	n.d.

For experimental details see Section 2.
n.d., value not determined.

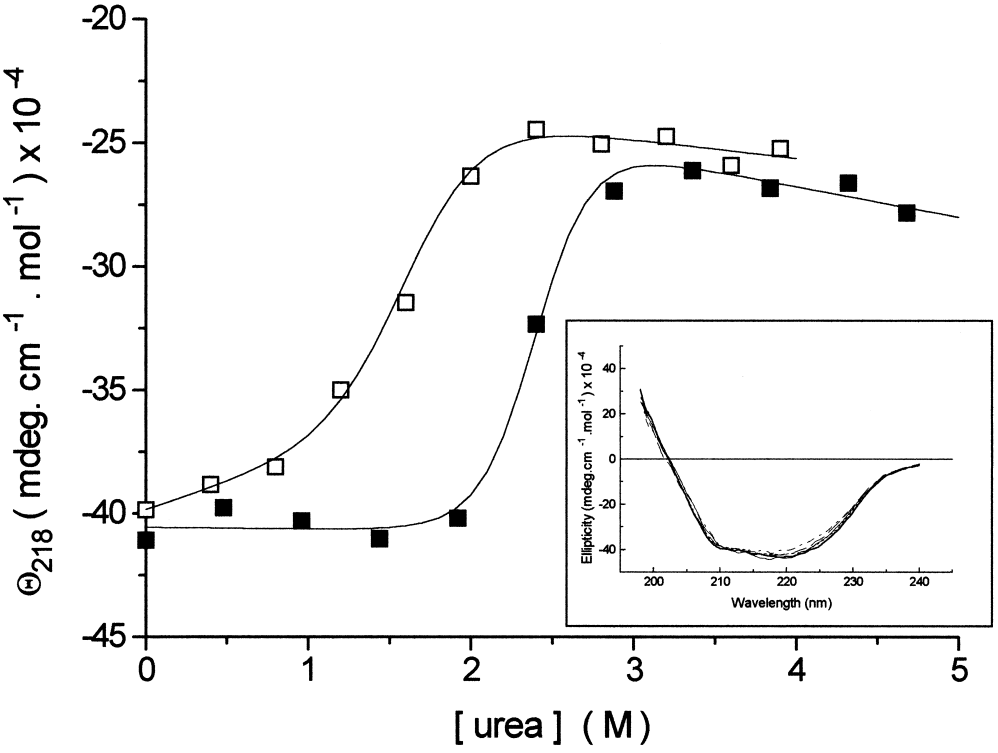

Fig. 2. Circular dichroism of αHL at 218 nm on titration with urea at pH 5.0 (■) and 7.0 (□). Inset shows the far-UV CD spectra of αHL in the absence of denaturant at pH 5.0 (dot-dashes), 5.5 (dashes), 6.0 (dots), 6.5 (long dashes) and 7.0 (solid line).

residues will alter the form of the final ITFE spectrum, which in turn will influence the value calculated for the spectral COM. The COM is therefore sensitive to changes in the microenvironments of all Trp residues such as might be found in intermediate conformations in the unfolding process; however, the monophasic transitions observed in Fig. 1 indicate the absence of such intermediates under the experimental conditions used in this study.

The changes in ITFE on unfolding of αHL were correlated with the changes in secondary structure as measured by CD at pH 5.0 and 7.0. The inset of Fig. 2 shows the far-UV CD spectra of αHL over the pH range 5.0–7.0 in the absence of urea, which are typical of a predominantly β-sheet protein in the native state and are similar to those described previously [20,25]. No changes in the far-UV CD spectra were observed in the absence of denaturant over the pH range used in this study. However, the main panel in Fig. 2 illustrates the effect of increasing concentrations of urea which result in a decrease in the ellipticity at 218 nm in buffers at both pH 5.0 and 7.0, with a transition at lower urea concentrations for pH 5.0. The solid lines in Fig. 2 show the results of the non-linear curve fitting of the ellipticity data, and the values derived for ΔG_u^{buff} and m_D from these fitted curves are shown in Table 1. The close correlation between the values of ΔG_u^{buff} and m_D derived from the CD and ITFE experiments indicates a concomitant loss of secondary and tertiary structure during the urea induced unfolding of αHL. The values of ΔG_u^{buff} derived from the non-linear curve fitting of the CD and ITFE data are presented in Fig. 3, where the solid line represents the least squares fit of the Henderson-Hasselbach equation to the data which yields a pK_a value of 6.2.

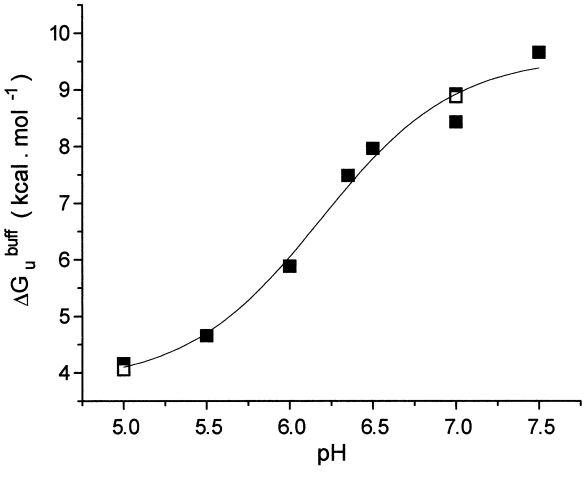

Fig. 3. Free energy of unfolding in buffer (ΔG_U^{buff}) of αHL as a function of pH. Values for ΔG_U^{buff} derived from non-linear least squares fitting of both ITFE (■) and CD (□) unfolding curves are shown. The solid line represents curve fitting of the data using the Henderson-Hasselbach equation with a pK_a of 6.2.

The changes in the secondary and tertiary structure of the αHL during urea-induced unfolding were correlated with changes in the elution time in SEC. At pH values of 5.0 and 7.0, increasing concentrations of urea from 0 to 6 M result in a decrease in the elution times for the αHL from ~31 min to ~27 min, with distinct pH-dependent transition regions. These changes are indicative of an increase in hydrodynamic radius, and the normalized elution times at pH 5.0 and 7.0 are presented in Fig. 4 together with the normalized CD and ITFE data as a function of urea concentration. The coincidence of the transition regions measured using CD and ITFE is matched by the transition measured by SEC, demonstrating that the loss of secondary and tertiary structure and

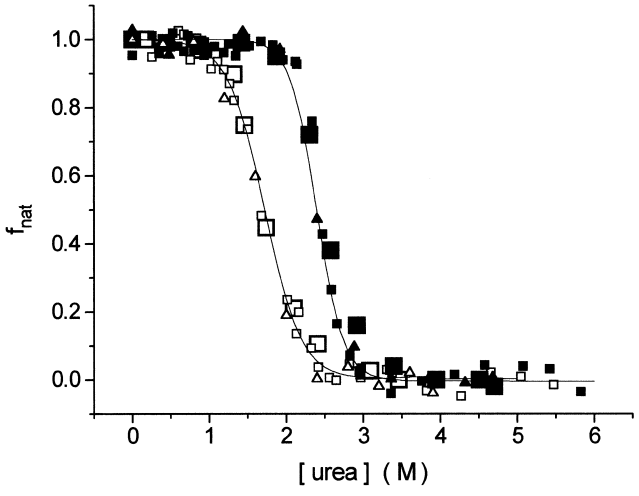

Fig. 4. Fraction of native protein (f_{nat}) as a function of urea concentration at pH 5.0 (open symbols) and 7.0 (solid symbols) as estimated by ITFE (small squares), CD (small triangles) and SEC (large squares). Values for f_{nat} were calculated as previously described [26]. The solid lines represent the curves derived from the ITFE data using values for ΔG_U^{buff} and m_D given in the text for pH 5.0 and 7.0 respectively.

the increase in the hydrodynamic radius are concomitant events. Although a slight divergence of the SEC data is observed in the final phase of the transition region, as shown in Table 1 the $[urea]_{50}$ values (the concentration of urea required for 50% denaturation) from all three techniques is comparable.

4. Discussion

Membrane damaging activity of the αHL is the consequence of the formation of a transmembrane pore, a process which has been extensively studied in vitro through the investigation of the interaction of the protein with artificial membranes (e.g. [3] for recent review). Consequently, a detailed model of pore formation has emerged in which the initial membrane association event is followed by a sequence of conformation changes terminating in the formation of a fully lytic heptamer. Although much information is available concerning the structural changes during the pore-forming process, investigation of the physico-chemical factors which influence the conformation transitions in the αHL have received little attention. In this study, we have evaluated the effect of changes in pH over a physiological range on the stability of the native state of the αHL through changes in the free energy of unfolding in buffer (ΔG_u^{buff}). We have demonstrated that for a decrease in the pH over the range calculated for the approach and association of αHL to a biological membrane, the ΔG_u^{buff} of the protein is significantly reduced from 8.9 to 4.2 kcal mol^{-1}. Furthermore, in the absence of denaturant the ITFE and CD spectra confirm that the reduction in protein stability induced by the lowered pH is not accompanied by detectable alterations in either the secondary or tertiary structure. These results are in accord with recent differential scanning calorimetry studies, which show that the melting temperature for the αHL decreases as the pH is reduced from 7.0 to 5.0 [28].

These observations may be correlated with the crystal structures of αHL [17] and two other pore-forming toxins, staphylococcal LukF [29,30] and protective antigen (PA) from *Bacillus anthracis* [31]. It is proposed that in the membrane associated PA pre-pore, mildly acidic pH facilitates the refolding of a greek key motif to form an extended β-hairpin structure, the tip of which traverses the membrane to form the walls of a heptameric transmembrane pore [31,32]. Direct evidence of a similar structural change in αHL has been obtained by comparison of the individual subunits in the final heptamer structure with that of the monomeric form of the structurally similar LukF [29,30]. In the case of PA, the loops and the β-strands which are proposed to undergo conformational change are rich in histidine residues, and the crystal structure of PA at mildly acidic pH demonstrates that a surface loop in this region becomes disordered [31]. It is noteworthy that the LukF and αHL were crystallized at neutral [30] and slightly acidic [7,17] pH respectively, and a comparison of the two structures reveals that although the secondary and tertiary structure of the rim domain is essentially unaltered, the polypeptide backbone atoms in this region of the αHL structure display elevated crystallographic *B*-factor values. This demonstrates an increased mobility of this region in the αHL as compared to LukF and although crystal packing effects cannot be excluded, it may suggest a correlation between decreased pH of the crystallization conditions and increased protein flexibility.

Previous studies have demonstrated that in solution at pH≦4.5 the α-helical pore-forming domains of several bacterial pore-forming toxins, including colicins [33,34], exotoxin A [35] and diphtheria toxin [36], adopt partially unfolded and more flexible conformations which are reminiscent of 'molten globule' states. It has been suggested that upon association of these proteins with biological membranes, the reduced local pH triggers the formation of a partially unfolded state which is functionally associated with the pore-forming process [37]. On the basis of conformation changes observed over the pH range 3.5–4.0 both in solution and on association of the protein with liposome membranes with high negative charge densities, a similar mechanism has been proposed for the αHL [20,38]. However, αHL retains pore-forming ability at pH 7.0 on liposome membranes with neutral net charge [39], where a model based on a pH-triggered conformation change predicts that the local pH at the membrane surface is similar to the bulk phase and would prevent formation of a partially unfolded state. Nevertheless, recent ITFE studies have obtained evidence consistent with the formation of an intermediate with altered tertiary structure on membranes with net neutral surface charge at pH 7.0 [25].

Results from these previous studies and those presented here would seem to imply that membrane binding rather than pH change over the physiological range triggers conformation change in αHL. However, pH does influence the rate of pore formation as demonstrated by conductance experiments using αHL on planar bilayers of lipids with neutral net charge [6,40], in which the maximum rate of pore formation occurs at bulk solvent pH values of 5.0–5.5, and decreases rapidly between pH 6.0 and 7.0 [40]. These results show a striking correlation with the pH values over which we observe the transition in ΔG_u^{buff}, and the least squares fitting to the Henderson-Hasselbach equation for the values of ΔG_u^{buff} yields a pK_a value of 6.2 which coincides with the protonation of the imidazole side chain of histidine residues. Indeed, site-directed mutagenesis studies of each of the four histidines in αHL have identified His35 and His48 as essential

residues for the correct oligomerization of the heptameric prepore and for subsequent pore formation [41–44]. We suggest that the reduced local pH in the vicinity of the membrane surface results in the protonation of key residues (possibly histidines) which leads to a reduction in the stability of the αHL. The reduced stability lowers free energy barriers between intermediate conformations of the protein with the consequent modulation of the rate of pore formation.

Acknowledgements: We are grateful to Dr. L.M. Beltramini for access to the spectropolarimeter at the Instituto de Física de São Carlos, Prof. S. Bhakdi (Institute of Medical Microbiology and Hygiene, Mainz, Germany) for providing *S. aureus* strain DU1090 transformed with plasmid pDU1212 and to Drs. R.E. Larson and N. Monesi for critical reading of the manuscript. R.K.B. was the recipient of FAPESP fellowship 94/1581-4. Financial support provided by FUNDUNESP Grant 533/94-DFP/F/CET and CNPq Grant 520082/95-8.

References

[1] Thelestam, M. and Blomqvist, L. (1988) Toxicon 26, 51–65.
[2] Bhakdi, S. and Tranum-Jensen, J. (1991) Microbiol. Rev. 55, 733–751.
[3] Bhakdi, S., Bayley, H., Valeva, A., Walev, I., Walker, B., Kehoe, M. and Palmer, M. (1996) Arch. Microbiol. 165, 73–79.
[4] Walker, B., Krishnasastry, M., Zorn, L. and Bayley, H. (1992) J. Biol. Chem. 267, 21782–21790.
[5] Feng, Y., Cheley, S., Bayley, H. and Yang, J. (1997) Biochemistry 36, 9518–9522.
[6] Walker, B., Krishnasastry, M., Zorn, L., Kasianowicz, J. and Bayley, H. (1992) J. Biol. Chem. 267, 10902–10909.
[7] Gouaux, J.E., Braha, O., Hobaugh, M.R., Song, L., Cheley, S., Shustak, C. and Bayley, H. (1994) Proc. Natl. Acad. Sci. USA 91, 12828–12831.
[8] Bhakdi, S., Fussle, R. and Tranum-Jensen, J. (1981) Proc. Natl. Acad. Sci. USA 78, 5475–5478.
[9] Valeva, A., Weisser, A., Walker, B., Kehoe, M., Bayley, H., Bhakdi, S. and Palmer, M. (1996) EMBO J. 15, 1857–1864.
[10] Walker, B., Krishnasastry, M. and Bayley, H. (1993) J. Biol. Chem. 268, 5285–5292.
[11] Walker, B. and Bayley, H. (1994) Protein Eng. 7, 91–97.
[12] Bayley, H. (1994) J. Cell. Biochem. 56, 177–182.
[13] Walker, B., Kasianowicz, J., Krishasastry, M. and Bayley, H. (1994) Protein Eng. 7, 655–662.
[14] Walker, B., Braha, O., Cheley, S. and Bayley, H. (1995) Chem. Biol. 2, 99–105.
[15] Ward, R.J. and Leonard, K. (1992) J. Struct. Biol. 109, 129–141.
[16] Ward, R.J., Palmer, M., Leonard, K. and Bhakdi, S. (1994) Biochemistry 33, 7477–7484.
[17] Song, L., Hobaugh, M.R., Shustak, C., Cheley, S., Bayley, H. and Gouaux, E. (1998) Science 274, 1859–1866.
[18] Cevc, G. (1990) Biochim. Biophys. Acta 1031, 311–382.
[19] Olivotto, M., Arcangeli, A., Carlà, M. and Wanke, E. (1996) BioEssays 18, 495–504.
[20] Vécsey-Semjén, B., Lesieur, C., Möllby, R. and van der Goot, F.G. (1997) J. Biol. Chem. 272, 5709–5717.
[21] McLaughlin, S. (1977) Curr. Top. Membr. Transp. 22, 407–421.
[22] Kraayenhof, R., Sterj, G.J. and Sang, H.W.W.F. (1993) Biochemistry 32, 10057–10066.
[23] Peitzsch, R.M., Eisenberg, M., Sharp, K.A. and McLaughlin, S. (1995) Biophys. J. 68, 729–738.
[24] Eisenberg, M., Gresalfi, T., Riccio, T. and McLaughlin, S. (1979) Biochemistry 18, 5213–5223.
[25] Bortoleto, R.K., de Oliveira, A.H.C., Ruller, R., Arni, R.K. and Ward, R.J. (1998) Arch. Biochem. Biophys. 351, 47–52.
[26] Pace, N. (1986) Methods Enzymol. 131, 266–279.
[27] Santoro, M.M. and Bolen, D.W. (1988) Biochemistry 27, 8063–8068.
[28] Vecsey-Semjen, B., Knapp, S., Möllby, R. and van der Goot, F.G. (1999) Biochemistry 38, 4296–4302.
[29] Olson, R., Nariya, H., Yokota, K., Kamio, Y. and Bouaux, E. (1999) Nature Struct. Biol. 6, 134–140.
[30] Pedelacq, J.D., Maveyraud, L., Prevost, G., Baba-Moussa, L., Gonzalez, A., Courcelle, E., Shephard, W., Monteil, H., Samama, J.P. and Mourey, L. (1999) Structure (London) 7, 277–284.
[31] Petosa, C., Collier, R.J., Klimpel, K.R., Leppla, S.H. and Liddington, R.C. (1997) Nature 385, 833–838.
[32] Benson, E.L., Huynh, P.D., Finkelstein, A. and Collier, R.J. (1998) Biochemistry 37, 3941–3948.
[33] Merrill, A.R., Cohen, F.S. and Cramer, W.A. (1990) Biochemistry 29, 5829–5836.
[34] van der Goot, F.G., Gonzalez-Manas, J.M., Lakey, J.H. and Pattus, F. (1991) Nature 354, 408–410.
[35] Jiang, J.X. and London, E. (1990) J. Biol. Chem. 265, 8636–8641.
[36] Zhao, J.M. and London, E. (1986) Proc. Natl. Acad. Sci. USA 83, 2002–2006.
[37] London, E. (1992) Mol. Microbiol. 6, 3277–3282.
[38] Vécsey-Semjén, B., Möllby, R. and van der Goot, F.G. (1996) J. Biol. Chem. 271, 8655–8660.
[39] Tomita, T., Watanabe, M. and Yasuda, T. (1992) Biochim. Biophys. Acta 1104, 325–330.
[40] Krasilnikov, O.V., Capistrano, M.P., Yuldasheva, L.N. and Nogueira, R.A. (1997) J. Membr. Biol. 156, 157–172.
[41] Jursch, R., Hildebrand, A., Hobom, G., Tranum-Jensen, J., Ward, R., Kehoe, M. and Bhakdi, S. (1994) Infect. Immun. 62, 2249–2256.
[42] Krishnasastry, M., Walker, B., Braha, O. and Bayley, H. (1994) FEBS Lett. 356, 66–71.
[43] Menzies, B.E. and Kernodle, D.S. (1994) Infect. Immun. 62, 1843–1847.
[44] Walker, B. and Bayley, H. (1995) Protein Eng. 8, 491–495.